Tuning the selectivity to aldehyde *via* pH regulation in the photocatalytic oxidation of 4-methoxybenzyl alcohol and vanillyl alcohol by TiO_2 catalysts

Sedat Yurdakal[a]*, Bilge Sina Tek[a], Çağlar Değirmenci[b], Giovanni Palmisano[c,d], Marianna Bellardita[e], Vittorio Loddo[e], Leonardo Palmisano[e], Javier Soria[f], Jesus Sanz[g], Vincenzo Augugliaro[e]*

[a]Kimya Bölümü, Fen-Edebiyat Fakültesi, Afyon Kocatepe Üniversitesi, Ahmet Necdet Sezer Kampüsü, 03200, Afyon, Turkey

[b]Kimya Bölümü, Fen Fakültesi, Eskişehir Teknik Üniversitesi, Yunus Emre Kampüsü, 26470, Eskişehir, Turkey

[c]Department of Chemical Engineering, Khalifa University of Science and Technology, P.O. Box 127788, Abu Dhabi, United Arab Emirates

[d]Research and Innovation Center on CO_2 and H_2, Khalifa University of Science and Technology, P.O. Box 127788, Abu Dhabi, United Arab Emirates

[e]"Schiavello-Grillone" Photocatalysis Group, Dipartimento di Ingegneria, Università degli Studi di Palermo, Viale delle Scienze (ed. 6), 90128 Palermo, Italy

[f]Instituto de Catálisis y Petroleoquímica, CSIC, C/ Marie Curie 2, Cantoblanco, 28049 Madrid, Spain

[g]Instituto de Ciencia de Materiales, CSIC, C/ Sor Juana Inés de la Cruz, Cantoblanco, 28049 Madrid, Spain

Abstract

The influence of pH on the photocatalytic partial oxidation of 4-methoxybenzyl alcohol (MBA) and vanillyl alcohol (VA) to their corresponding aldehydes in aqueous suspension was investigated by using poorly crystalline home-prepared (HP) and crystalline commercial TiO_2 (BDH, Merck and Degussa P25) photocatalysts. The results clearly show as tuning pH can strongly impart selectivity to photocatalytic processes which are often quite unselective in aqueous suspensions. It has been found that pH effect on reaction rate and product selectivity strongly depends on TiO_2 crystallinity and substrate type. Notably, the first order kinetic constant values in the presence of crystalline Merck and BDH TiO_2 catalysts were generally high at very high pH's by oxidising both MBA (i.e. $2.65x10^{-4}$ $mM \cdot h^{-1} \cdot m$ for Merck and $2.22x10^{-4}$ $mM \cdot h^{-1} \cdot m$ for BDH at pH 13) and VA (i.e. $1.20x10^{-4}$ $mM \cdot h^{-1} \cdot m$ for Merck and $1.63x10^{-4}$ $mM \cdot h^{-1} \cdot m$ for BDH at pH 13). Conversely, the use of poorly crystallized HP samples gave rise to high k values at low pH's. High selectivity values (up to 100%) for MBA oxidation were obtained at low pH's (1-2), whereas selective VA oxidation (up to 39%) was achieved at high pH's (10-13) by using both HP and commercial TiO_2 photocatalyts.

Additional experiments starting from the products demonstrated that the selectivity depended on the resistance of these compounds to over-oxidation under the experimental conditions used.

Keywords: TiO_2; pH effect; photocatalysis; p-anisaldehyde; vanillin; green synthesis.

1. Introduction

In the last years, synthetic photocatalysis, performed under mild and environmentally friendly conditions, has attracted a lot of attention to convert traditional processes that often operate under drastic experimental conditions into green processes [1]. As a result, there is a global need for a productive, competitive, energy and resource efficient economy in the field of chemical process sustainability, reducing by-products and hazardous wastes, such as toxic organic solvents and hardly disposable metal catalysts. A new synthetic organic catalytic [2-5] and photocatalytic [6-8] Chemistry has been recently developed, aiming to carry out reactions in water, and it was undoubtedly proved that several chemical reactions can take place in aqueous solvents, by reaching high reaction rate and selectivity even for insoluble reagents. However, it should be remembered that some green photocatalytic processes described in literature and concerning the formation of high added value chemicals, although if highly innovative, cannot be strictly defined as "synthesis processes" because the product(s) has(have) not been separated from the reaction environment and purified, as generally occurs in Organic Chemistry. Consequently, further studies and possibly the scale-up of the processes are necessary also from an engineering point of view, also evaluating their feasibility from an economic point of view. Oxidation of alcoholic to carbonyl group is an important reaction commonly employed in the synthesis of compounds of industrial interest [9]. The development of oxidation processes making use of clean oxidants and stable and atoxic catalysts is of great concern [10].

TiO_2-based photocatalysis is an advanced technology mainly used for water and air purification [11-14]. However, a growing number of studies on selective oxidations [15-25] have also been made. Several primary and secondary alcohols have been selectively oxidised in gas-solid systems [21] by using an immobilised catalyst; and in particular aryl alcohols have been oxidized to the corresponding aldehydes, ketons and acids in acetonitrile solvent [22]. Palmisano et al. [23,24] reported the photocatalytic oxidation of aromatic alcohols to aldehydes in aqueous suspensions and in fixed-beds of home-prepared TiO_2 catalysts. The different behaviour of poorly crystallized home-prepared catalysts compared to commercial crystalline ones was studied and the former were much more selective [23-25].

The influence of aromatic ring substituents on selectivity was also investigated for different 4-substituted aromatic alcohols in the presence of home prepared rutile TiO_2 [25], finding that an electron donor group gives rise to both higher activity and selectivity. The hydroxylation of phenol and benzoic acid in water by using different TiO_2 samples showed that the selectivity toward the mono-hydroxy derivatives depends on the photocatalysts features as

crystallinity and hydroxylation degrees, in particular the best results were observed when commercial very crystalline and poorly hydroxylated samples were employed [26].

In the present investigation the photocatalytic oxidation of MBA and VA to *p*-anisaldehyde (PAA) and vanillin (VAN) has been studied at various pH's to understand how the conversion of the above substrates and their selectivity is influenced by changing the pH. Different commercial (TiO_2 Merck, BDH and Degussa P25) and home-prepared ex-$TiCl_4$ catalysts have been used. Notably, the two obtained aldehydes are of huge interest by an industrial point of view. *p*-Anisaldehyde is indeed a species used in flavour compositions for confectioneries and beverages, as well as being an important chemical intermediate of pharmaceuticals, agrochemicals, dyes and plastic additives [27]. On the other hand, the use of vanillin is extensive in food, cosmetic, pharmaceutical, nutraceutical and fine chemical industry [28].

2. Experimental part

2.1 Preparation of HPRT

The solution of the precursor was obtained by adding 20 mL of $TiCl_4$ (>97%, Fluka) to 1000 mL of water contained in a volumetric flask (500 mL) [25]. The addition was carried out drop-wise under continuous magnetic agitation by maintaining the flask in an ice bath. At the end, the resulting solution was stirred for 2 min by a magnetic stirrer, and then the flask was sealed and kept at room temperature (ca. 298 K) for an aging time of 6 days. The solid powder, precipitated at the end of the whole treatment, was separated by centrifugation (20 min at 5000 rpm) and dried at room temperature. The final home-prepared catalyst is hereafter indicated as HPRT.

2.2 Preparation of HP0.5

The details of catalyst preparation are reported elsewhere [15]. The precursor solution was obtained by adding 20 mL of $TiCl_4$ (purity >97%, Fluka) to 200 mL of deionized water contained in a 500 mL beaker. The addition was made drop-wise under continuous magnetic agitation and carried out inside an ice bath. After that, the beaker was sealed, and mixing was prolonged for 12 h at room temperature, eventually obtaining a clear solution. A volume of 125 mL of the resulting solution was put inside a 250 mL round-bottomed flask fitted with a Graham condenser. The flask was heated at 373 K, magnetically stirred, and refluxed for 0.5 h; the reflux time count started when the solution lost its transparency. The obtained suspension was then

dried at 323 K by means of a rotary evaporator (Buchi model M) working at 150 rpm in order to obtain the final powdered catalysts. The final home prepared catalyst is hereafter indicated as HP0.5.

2.3 Samples characterization

X-Ray diffraction (XRD) analysis of the powders was performed by a Philips diffractometer (operating at a voltage of 40 kV and a current of 30 mA) using the CuKα radiation and a 2θ scan rate of 1.28° min^{-1}. The crystallite size of the samples was determined by using the Scherrer equation [29].

The specific surface areas (SSA) of the powders were determined in a FlowSorb 2300 apparatus (Micromeritics) by using the single-point BET method. The samples were degassed for 0.5 h at 523 K prior to the measurement by using a N_2/He mixture 30/70 v/v.

Particles agglomerates were evaluated by SEM images, obtained by using an ESEM microscope (Philips, XL30) operating at 25 kV. A thin layer of gold was evaporated on the catalysts samples, previously sprayed on the stab and dried at room temperature.

2.4. Photocatalytic set-up and procedure

The photoreacting system consisted of a continuously stirred (ca. 400 rpm) cylindrical photocatalytic reactor (CPR). The CPR (inner tube diameter: 32 mm; height: 188 mm) was irradiated by three fluorescent lamps (Philips, 8 W) axially placed and emitting in the near-UV region at 365 nm. The total volume of the suspension was 150 mL. The catalyst amount used was 0.40 g L^{-1} in pure aqueous solvent, whereas the initial concentration of both MBA and VA was 0.50 mM. The pH of the solution was adjusted by using 1M HCl and 1M NaOH solutions.

Before switching on the lamp, the solution was stirred for 30 min at room temperature to reach the thermodynamic equilibrium. Before and during the runs the aqueous solution was in contact with atmospheric air, thus absorbing oxygen from the environment. Adsorption of the organic substrate on the photocatalyst surface was negligible under dark. During the run, samples were withdrawn from the solution at fixed time intervals. The quantitative determination and identification of the species present in the solution was performed by means of a Beckman Coulter HPLC (System Gold 126 Solvent Module and 168 Diode Array Detector), equipped with a Phenomenex, Kinetex 5 μm C18 100A column (4.6 mm × 150 mm) and working at room temperature. The eluent consisted of 20% acetonitrile and 80% 13 mM trifluoroacetic acid aqueous solution and its flow rate was 0.8 cm^3 min^{-1}. Retention times and UV spectra of the compounds were compared with those of standards. Total organic carbon

(TOC) analyses were carried out by using a 5000 A Shimadzu analyser in order to evaluate the degree of mineralization. All of the used chemicals were purchased from Sigma Aldrich with a purity >98.0%.

3 Results and Discussion

3.1 Catalysts characterization

X-ray diffractograms of all the catalytic samples are reported in Figure 1. Peaks at 2θ = 27.5°, 36.5°, 41°, 54.1° and 56.5° are characteristic of rutile and those at 2θ = 25.5°, 38.0°, 48.0°, 54.5° of anatase. Table 1 shows the main features of the catalysts. The crystallinity degree was previously determined [17]. The various peaks corresponding to the two main phases of TiO_2 have been identified. The two commercial samples Merck and BDH consist of pure anatase TiO_2, the HPRT and HP0.5 diffractograms show the presence of rutile and anatase as the main phase, respectively. The average crystallite diameters of the commercial samples (29-60 nm), estimated by means of the Scherrer's equation, are much higher than those of the home-prepared ones (ca. 6 nm).

The commercial samples are the most crystalline ones (56-90 %), the crystallinity of the home prepared samples (ca. 10%), HPRT and HP0.5, is instead very poor, since their synthesis took place at low temperature (25 and 100 °C, respectively). In Table 1 it is possible to observe that the specific surface areas (SSA) of the home prepared samples are one order of magnitude higher than those of the commercial ones, whereas the crystallite sizes are smaller.

Figure 2 shows SEM images of home-prepared and commercial TiO_2 catalysts. The small SSA of BDH and Merck indicate a strong particle agglomeration (120 and 170 nm, respectively) confirmed by SEM images.

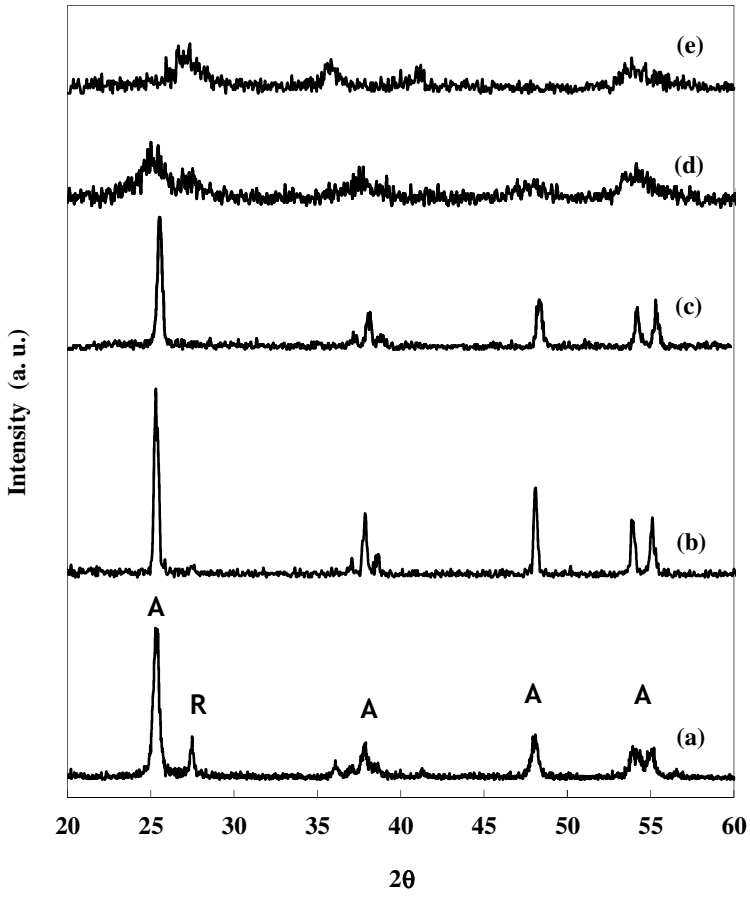

Figure 1. XRD patterns of the samples: (a) P25; (b) Merck; (c) BDH; (d) HP0.5; (e) HPRT.

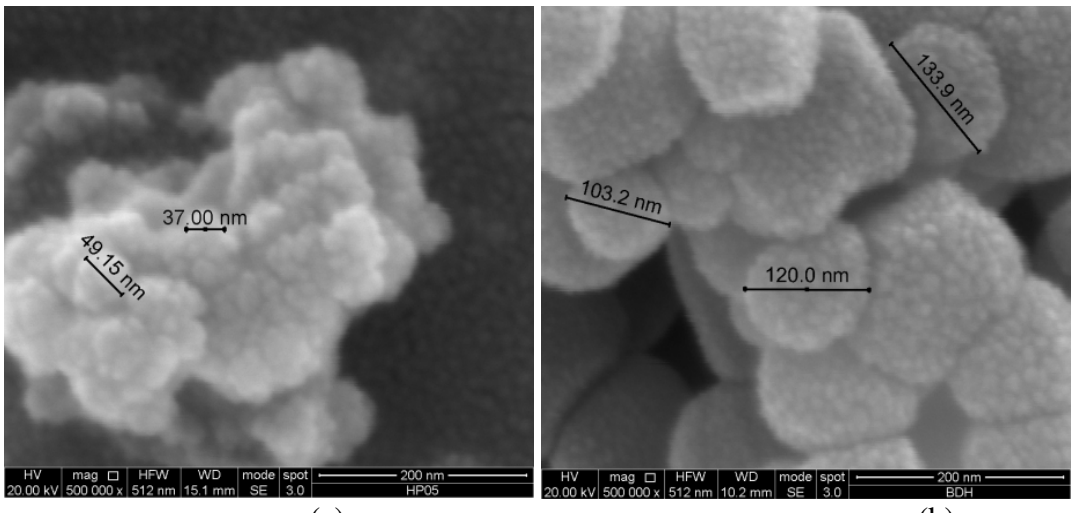

(a) (b)

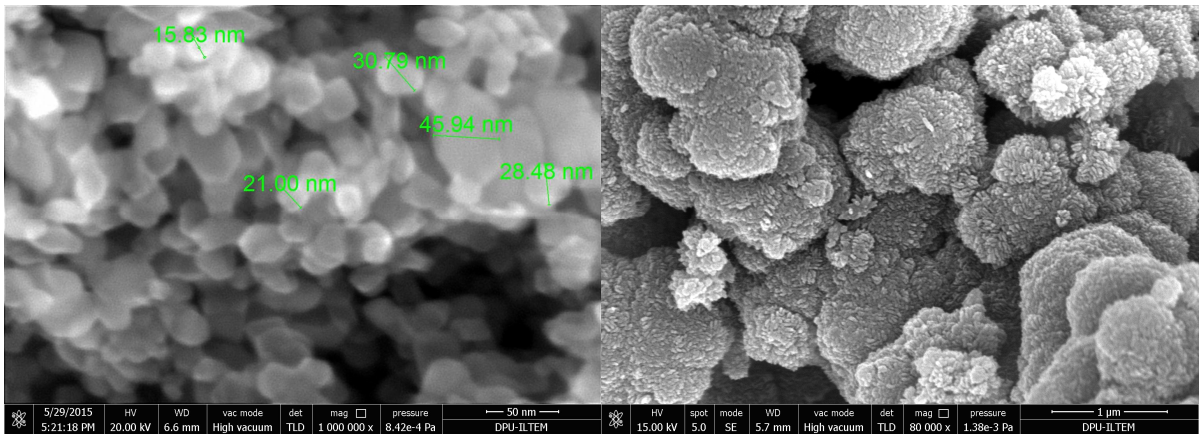

(c) **(d)**

Figure 2. SEM images of: (a) HP0.5; (b) BDH; (c) Degussa P25; (d) HPRT

Table 1. Crystalline phases (A: anatase; R: rutile), crystallinity, BET specific surface areas (SSA), agglomerate and crystallite sizes of the used photocatalyts.

Catalyst	Crystalline phase	Crystallinity (%)	SSA (m^2 g^{-1})	Crystallite size (nm)
HPRT	R	negligible	118	7
HP0.5	A+R	10	155	5
BDH	A	56	11	35
Merck	A	74	11	60
Degussa P25	A+R	90	50	29

3.2. Photoactivity results

The oxidation of MBA and VA was followed by measuring the concentration of alcohols, aldehydes (p-Anisaldehyde (PAA) and vanillin (VAN)) and CO_2 that were the main reaction products. The degree of mineralization related to CO_2 concentration, was extrapolated from the TOC values, provided that no organic volatile species formed during the reaction. Homogeneous runs were carried out in the absence of catalyst at different pH's and the activity was found to be low (ca. 8% conversion after 3h irradiation at pH 1) with respect to all of the heterogeneous ones. Similar results were obtained in the presence of SiO_2, a non-photoactive sample (see Table 2). It was also verified that reactions did not take place in the absence of either light or oxygen.

Experiments were carried out at different pH's, ranging from 1 to 13, and the experimental results and kinetic parameters (zero or first order rate constants) are reported in Tables 2-4 for MBA and VA, respectively.

Zero (Eq.1) or first (Eq.2) order rate constants (k) have been calculated by the following

equations [30]:

$$(-r_0) = -\frac{1}{S}\left(\frac{dN}{dt}\right) = -\frac{V}{S}\left(\frac{dC}{dt}\right) = k \quad (1)$$

$$(-r_0) = -\frac{1}{S}\left(\frac{dN}{dt}\right) = -\frac{V}{S}\left(\frac{dC}{dt}\right) = kC \quad (2)$$

where $-r_0$ indicates the initial rate constants, N the moles of substrate, *t* the irradiation time (h), S the specific surface area (m^2/g), V the suspension volume (m^3), and *C* (mM) the substrate concentration. The calculated kinetic rate constants of pseudo-first order (k) show a good fitting especially at pH 5 and higher. At pH 1 (and sometimes at pH 2), the reactions fit zero order reaction kinetics.

By analysing selectivity at 15 and 50 % MBA conversion, it can be seen how high figures (57-100%) were obtained at very acidic media (pH=1 and pH=2), whereas very low selectivity values were observed (12-36 %) at pH=5÷13 by using both HP and commercial TiO_2 photocatalyts. 100% Selectivity at 50% MBA conversion was obtained by using HP0, that is the worst crystalline sample (Table 2). At 100% MBA conversion, moreover, selectivity remained still quite high (78%). Generally, the oxidizing capacity of a photocatalyst is greater as the crystallinity increases because the ordered crystal lattice decreases the degree of recombination of the charge. Interestingly, the structure of HP0.5 is poorly crystalline and its selectivity not so high even at pH 1 (57%). HP0.5 is mainly in anatase phase, whilst HPRT consists mainly of rutile. This result shows that poorly crystallized rutile TiO_2 catalysts are more suitable than anatase ones for selective MBA oxidation at low pH values.

The highest first order kinetic constant values were given by Merck, BDH and Degussa P25 samples at pH 13. However, under these conditions, selectivity values towards PAA are very low, 22, 27 and 30 %, respectively.

Notably, a decrease of pH resulted in an increase of both activity and selectivity towards PAA in the presence of home-prepared samples (Figure 3 and 4), whereas activity was higher at high pH's by using commercial catalysts different from Degussa P25 (Figure 4). The former behaviour is of strong interest, because it demonstrates that a simple tuning of pH can improve selectivity without negatively affecting activity for poorly crystalline catalysts. Commercial Merck and BDH behaved instead differently, since a decrease of pH yielded an increase of selectivity, with a contemporary decrease of activity.

It was expected that the crystalline samples were very active at basic pH, due to the increased formation of hydroxyl radicals coming from hydroxyl anions in these conditions. It

has been demonstrated that not all the surface hydroxy groups are transformed into hydroxyl radicals under irradiation, and the amount of hydroxyl radicals is higher for commercial well crystallized samples [31]. This finding explains the higher photoactivity of commercial TiO_2 samples at basic pH's, although their OH surface density resulted smaller than that of the home prepared samples. Nevertheless, agglomeration of catalyst particles is generally known to occur strongly in a basic environment, and this phenomenon can negatively affect the MBA oxidation rate, because of the decrease of the number of the active surface sites. Therefore, the activity depends on both hydroxyl radical concentration produced throughout the experiments and catalyst agglomeration degree. By considering these two related effect and the used experimental conditions, we can hypothesise that agglomeration effect is predominant in poorly crystallized/almost amorphous samples. Consequently, HP samples showed very low MBA oxidation rate at pH 13. For instance, at pH=5 and pH=13, HPRTshowed just 10 % conversion after 2h and 3h irradiation, respectively. Home-prepared catalytic particles can agglomerate easily at basic pH's because their amorphous surface is significantly hydroxylated. In other words, at very low pH's, very well dispersed suspensions and high activities were obtained in the presence of HP samples [32]. In addition, the activity of Degussa P25 decreases by increasing pH different from Merck and BDH. This event supports our hypothesis since the particle size of Degussa P25 increases by increasing the pH [32], different from the Merck sample, and the activity of Degussa P25 is lower than that of the other commercial catalysts at basic conditions.

Table 2. Photoreactivity results of MBA oxidation obtained at different pH values. MBA initial concentration: 0.50 mM; catalyst amount: 0.4 g·L^{-1}.

pH	Catalyst	S_{PAA} (%) $X_{0.15}$	S_{PAA} (%) $X_{0.50}$	X_{1h} (%)	X_{3h} (%)	1st →k (h^{-1}·m) x10^6 0th→ k (mM·h^{-1}·m) x10^6
1	-	10			7	
1	SiO_2	63			8	
1	BDH	90	84	40	96	92[a]
2	BDH	97	78	30	92	80[a]
5	BDH	40	18	25	65	150
10	BDH	31	17	40	71	181
13	BDH	33	27	60	83	222
1	Merck	80	78	22	100	88[a]
2	Merck	85	75	28	75	201
5	Merck	20	13	22	57	126
13	Merck	33	22	57	86	265
1	Degussa P25	81	88	100	100	127[a]
5	Degussa P25	30	12	37	70	34
13	Degussa P25	42	30	57	88	74
1	HPRT	100	100	82	100	21[a]
2	HPRT	95	90	34	85	6.4[a]
5	HPRT	78		5.8	12	1.8
13	HPRT	55		3.2	10	1.7
1	HP0.5	60	57	99	100	27[a]
5	HP0.5	39	29	14	36	4.6
13	HP0.5	40	36	23	43	5.7

k: zero ([a]) or first order kinetic constants. S_{PAA}: selectivity values towards p-anisaldehyde after 15% ($X_{0.15}$) and 50% ($X_{0.50}$) conversions. X_{1h} and X_{3h}: conversion values after 1h and 3h of reaction time, respectively.

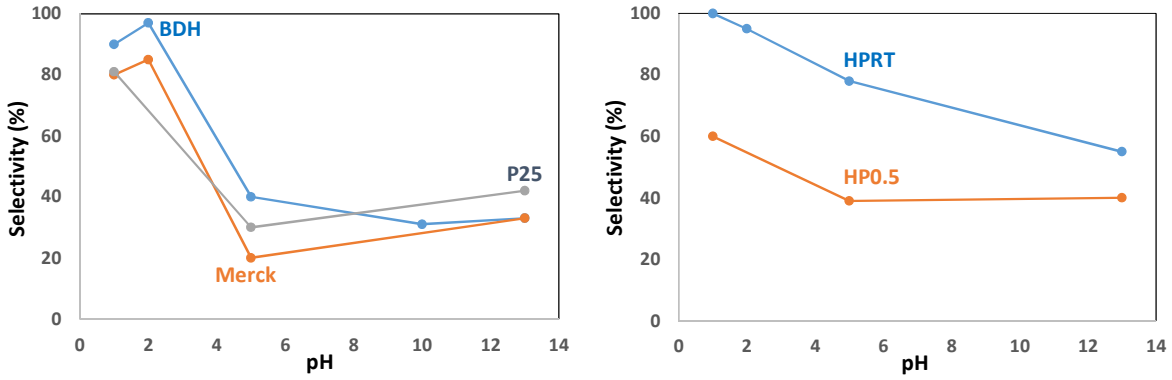

Figure 3. Selectivity *vs* pH values for the oxidation of MBA to PAA by using well crystallized (a) and poorly crystallized (b) catalysts. The used selectivity values were considered after 15% conversion.

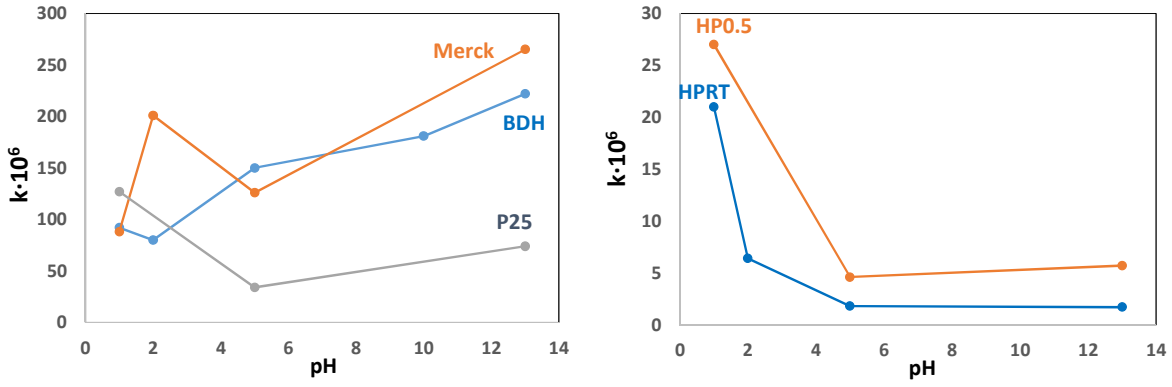

a) (b)

Figure 4. k *vs* pH values in the oxidation of MBA to PAA by using well crystallized (a) and poorly crystallized (b) catalysts.

Figure 5 shows representative photocatalytic runs where MBA was oxidized by Merck TiO_2 at different pH values. At pH 1, both MBA degradation and PAA production increase linearly, however at higher pH's (2-13) the increase is logarithmic. At pH 13, after 30 min, the amount of produced PAA did not increase, which is the reason of low PAA selectivity. Produced PAA was over-oxidised probably since it is unstable at high pH's. Furthermore, after 30 min, the reaction rate of MBA degradation decreases due to competition with the degradation of the PAA produced which becomes relevant due to a more significant presence of this molecule than in the initial stages of the reaction.

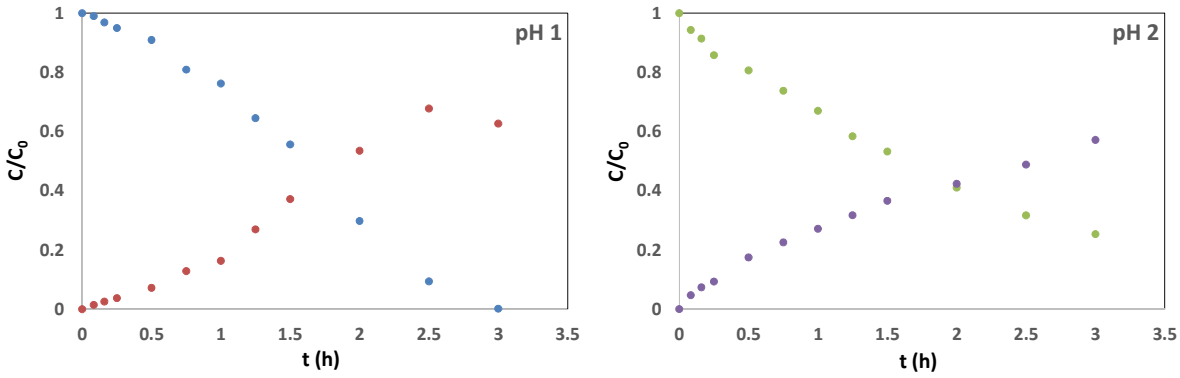

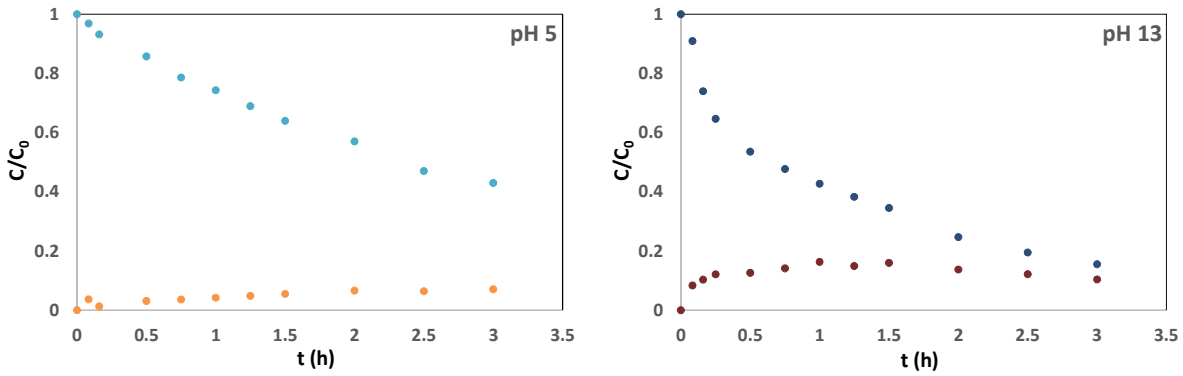

Figure 5. Experimental results of representative runs of MBA degradation and PAA production versus irradiation time by using Merck TiO_2 catalysts at pH 1, pH 2, pH 5 and pH 13.

The effect of different acids and ions on MBA oxidation was studied and the results obtained are shown in Table 3. The presence of HCl strongly influences both the selectivity and the activity with respect to H_2SO_4 and H_3PO_4. To evaluate the effect of Cl^-, the same experiments were also carried out in the presence of 0.1 M NaCl in the suspension, and the selectivity values were very low. These results indicate that selective oxidations are crucially influenced not only by the concentration of protons, but also by the counter-anion, at least in the case of hydrochloric acid and chloride ion.

Table 3. Photoreactivity results of MBA oxidation obtained at different pH values adjusted by different acid sources. MBA initial concentration: 0.5 mM; catalyst amount: 0.4 g L^{-1}. [HCl], [H_2SO_4], [H_3PO_4] = 0.1 M.

pH	Catalyst	Acid or salt sources	S_{PAA} (%) $X_{0.15}$	S_{PAA} (%) $X_{0.50}$	X_{3h} (%)
1	-	HCl	10	-	7
1	BDH	HCl	90	84	97
1	BDH	H_2SO_4	55	35	43
1	BDH	H_3PO_4	45	28	34
5	BDH	NaCl	22	15	59

S_{PAA}: p-anisaldehyde selectivities after 15% ($X_{0.15}$) and 50% ($X_{0.50}$) conversions. X_{3h}: conversion values after 3h of irradiation time. Concentrations of acids and NaCl: 0.1 M.

VA oxidation showed a rather different behaviour with respect to MBA (Table 4). Activity and selectivity to vanillin were in accordance with a previous work [33] and generally lower than that obtained for the oxidation of MBA. Therefore, the reported selectivity figures were determined just after 15 % conversion of VA. For instance, the selectivity towards vanillin reached an optimum value of 5.5 % after 15% conversion at pH 1 by using Merck as the catalyst (see Table 4), whereas MBA can be oxidised with 80% selectivity after the same time and pH. The k are generally higher for MBA oxidation than for VA. The important unselective oxidation of VA is due to the presence of a substituent group in *meta*-position [33], and it can be ascribed

to the presence of three different substituents on the aromatic ring, that can lead to a strong photoadsorption on the catalyst surface with an easy oxidation attack. The strong photoadsorption can moreover hinder a subsequent photodesorption of the reaction products, thus leading both to aliphatic intermediates coming from aromatic ring breakage and to mineralization. Conversely, MBA does not photoadsorb strongly on the catalyst and it is thus easily oxidised to PAA without ring breakage at low pH, probably due to the structure and properties of PAA.

Basic conditions enhance VAN selectivity very much with respect to acidic and intermediate pH's, by employing both commercial and home-prepared catalysts. This trend is specular to what reported for MBA (Table 2), where a lower selectivity was present at the intermediate and high pH's. Reaction rates instead decrease by decreasing pH in the presence of commercial samples, differently from home-prepared samples, that showed a minor dependence of reaction rate on pH.

Table 4. Photoreactivity results of VA oxidation obtained at different pH values. VA initial concentration: 0.5 mM; catalyst amount: 0.4 $g \cdot L^{-1}$.

pH	Catalyst	S_{VAN} (%) $X_{0.15}$	X_{1h} (%)	X_{3h} (%)	$1^{st} \rightarrow k$ ($h^{-1} \cdot m$) x10^6 $0^{th} \rightarrow k$ ($mM \cdot h^{-1} \cdot m$) x10^6
1	BDH	4.4	4	12	9.3[a]
5	BDH	12	26	65	159
10	BDH	28	20	40	64
13	BDH	35	44	69	163
1	Merck	5.5	7	13	7.9[a]
5	Merck	12	24	60	145
13	Merck	39	37	58	120
1	HPRT	3.7	12	27	4.0
5	HPRT	10	20	34	5.0
13	HPRT	14	9.2	18	2.8
1	HP0.5	6.0	14	33	1.7[a]
5	HP0.5	15	19	37	4.5
13	HP0.5	27	13	29	3.6

k: zero ([a]) or first order kinetic constants. S_{VAN}: vanillin selectivity after 15% ($X_{0.15}$) conversion. X_{1h} and X_{3h}: conversion values after 1h and 3h of irradiation time, respectively.

Selected runs were carried out in order to oxidise PAA at pH=1 and pH=13, in order to understand the low selectivity to PAA in basic environments. The corresponding results are reported in Table 5 and are quite surprising: heterogeneous reaction carried out by using BDH at pH=1 gives rise to a conversion value of 81%, while this is only 23% at pH=13 for 2h of irradiation. Therefore, during MBA oxidation at pH=1, the aldehyde over-oxidises very slowly upon its formation, allowing to reach very high selectivity values. Similarly homogeneous oxidation of PAA carried out at pH=13 gives rise to a conversion of 21%, whilst no oxidation was obtained at pH 1 for 2h of irradiation time.

VAN conversion value at pH 1 is ca. 2 times higher than that of pH 13 (44 vs 23%). Similarly, VAN oxidations were performed by using BDH and in homogenous conditions. In homogenous conditions and at pH 13, almost no conversion was observed, whereas it was 21% at pH 1.

Consequently, the selectivity towards the product mainly depends on the oxidation resistance of the molecule produced under the experimental conditions used (see Table 5).

Table 5. Photoreactivity results of p-anisaldehyde (PAA) and vanillin (VAN) oxidation obtained at different pH's. PAA and VAN initial concentrations: 0.5 mM; catalyst amount: 0.4 $g \cdot L^{-1}$.

pH	Catalyst	Substrate	X_{2h} (%)
1	BDH	PAA	20
1	Homogenous	PAA	-
13	BDH	PAA	81
13	Homogenous	PAA	21
1	BDH	VAN	44
1	Homogenous	VAN	21
13	BDH	VAN	23
13	Homogenous	VAN	-

X_{2h}: conversion values after 2h of reaction time.

Conclusion

In the present work, the effect of pH on partial aromatic alcohol oxidations was investigated for crystalline and poorly crystalline/almost amorphous TiO_2 photocatalysts. The obtained results show that the influence of pH on reaction rate and product selectivity strongly depends on TiO_2 crystallinity and substrate features. In MBA oxidations, at very low pH values (1-2), very high product selectivity values were obtained, whilst in VA oxidation, very basic conditions (i.e. 13) were favourable. k values, especially for MBA oxidation, are very much influenced by TiO_2 crystallinity; crystalline catalysts are very active at high pH, while the poorly crystalline/almost amorphous ones at low pH. The obtained results show that in the presence of a high concentration of HCl or NaOH the catalyst surface and consequently the adsorption-desorption equilibria of substrate and products and the size of TiO_2 particles changed. Furthermore, it was shown that the selectivity of the product was related to the resistance of the product to over-oxidation attacks in the experimental conditions used.

Acknowledgments

Dr. S. Yurdakal thanks the TÜBİTAK (Project no: 111T489) for financial support.

References

1. L. Palmisano, V. Augugliaro, M. Bellardita, A. Di Paola, E. García López, V. Loddo, G. Marcì, G. Palmisano, S. Yurdakal, ChemSusChem 4 (2011) 1431-1438.
2. J.E. Klijn, J.B.F.N. Engberts, Nature 435 (2005) 746-747.
3. C. Li, L. Chen, Chem. Soc. Rev. 35 (2006) 68-82.
4. S. Narayan, J. Muldoon, M.G. Finn, V.V. Fokin, H.C. Kolb, K. Barry Sharpless, Angew. Chem. Int. Ed. 44 (2005) 3275-3279.
5. G.B. Jacobson, C.T. Lee, Jr., S.R.P. da Rocha, K.P. Johnston, J. Org. Chem. 64 (1999) 1207-1210.

6. H. Yoshida, Photocatalytic Organic Syntheses. In: Anpo M., Kamat P. (eds) Environmentally Benign Photocatalysts. Nanostructure Science and Technology. Springer, 2010, New York, NY.
7. D. Friedmann, A. Hakki, H. Kim, W. Choi, D. Bahnemann, Green Chem. 18 (2016) 5391-5411.
8. F. Parrino, M. Bellardita, E.I. Garcia-López, G. Marcì. V. Loddo, L. Palmisano, ACS Catal. 8 (2018) 11191–11225.
9. B.M. Trost, I. Fleming, S.V. Ley (Eds.), Comprehensive Organic Synthesis (Vol. 7), Pergamon Press, Oxford, 1991.
10. T. Mallat, A. Baiker, Chem. Rev. 104 (2004) 3037-3058.
11. A. Fujishima, T.N. Rao, D.A. Tryk, J. Photochem. Photobiol. C 1 (2000) 1-21.
12. D. Sannino, V. Vaiano, O. Sacco, P. Ciambelli, J. Envir. Chem. Eng. 1 (2013) 56-60.
13. K.L. Wang, M. Endo-Kimura, R. Belchi, D. Zhang, A. Habert, J. Boucle, B. Ohtani, E. Kowalska, N. Herlin-Boime, Materials, 12, 4158.
14. V. Augugliaro, M. Litter, L. Palmisano, J. Soria, J. Photochem. Photobiol. C 7 (2006) 127-144.
15. G. Palmisano, S. Yurdakal, V. Augugliaro, V. Loddo, L. Palmisano, Adv. Synth. Catal. 349 (2007) 964-970.
16. A. Maldotti, A. Molinari, R. Amadelli, Chem. Rev. 102 (2002) 3811-3836.
17. M. Bellardita, V. Loddo, G. Palmisano, I. Pibiri, L. Palmisano and V. Augugliaro, Appl. Catal. B 144 (2014) 607-613.
18. K. Czelej, K. Cwieka, J. C. Colmenares, K. J. Kurzydlowski, Y.-J. Xu, ACS Appl. Mater. Inter., 9 (2017) 31825-31833.
19. M.A. Gonzalez, S.G. Howell, S.K. Sikdar, J. Catal. 183 (1999) 159-162.
20. T. Caronna, C. Gambarotti, L. Palmisano, C. Punta, F. Recupero, Chem. Commun. 18 (2003) 2350-2351.
21. U.R. Pillai, E. Sahle–Demessie, J. Catal. 211 (2002) 434-444.
22. O.S. Mohamed, A.E.M. Gaber, A.A. Abdel-Wahab, J. Photochem. Photobiol. A: Chem. 148 (2002) 205-210.
23. S. Yurdakal, G. Palmisano, V. Loddo, V. Augugliaro, L. Palmisano, J. Am. Chem. Soc. 130 (2008) 1568-1569.
24. V. Loddo, S. Yurdakal, G. Palmisano, G. E. Imoberdorf, H. A. Irazoqui, O. M. Alfano, V. Augugliaro, H. Berber, L. Palmisano, Int. J. Chem. React. Eng. 5 (2007) A57 (1-15).

25. S. Yurdakal, G. Palmisano, V. Loddo, O. Alagöz, V. Augugliaro, L. Palmisano, Green Chem. 11 (2009) 510-516.
26. M. Bellardita, V. Augugliaro, V. Loddo, B. Megna, G. Palmisano, L. Palmisano, M.A. Puma, Appl. Catal. A 441- 442 (2012) 79-89.
27. Flavors and Fragrances, in: Ullmann's Encyclopedia of Industrial Chemistry, (Release 2006, 7 th edn.), Wiley-VCH, Weinheim, and references cited therein.
28. H. Korthou, R. Verpoorte, Vanilla, Flavours and Fragrances, Springer, 2007.
29. P. Scherrer, Nachr. Ges. Wiss. Göttingen, Math. Phys. Kl. 2 (1918) 98-100.
30. F. Parrino, V. Loddo, V. Augugliaro, G. Camera-Roda, G. Palmisano, L. Palmisano, S. Yurdakal, Catal. Rev. Sci. Eng. 61 (2019) 163-213.
31. A. Di Paola, M. Bellardita, L. Palmisano, Z. Barbierikova, V. Brezová, J Photochem Photobiol A 273 (2014) 59–67.
32. S. Yurdakal, V. Loddo, B.B. Ferrer, G. Palmisano, V. Augugliaro, J. Giménez Farreras, L. Palmisano, Ind. Eng. Chem. Res. 46 (2007) 7620-7626.
33. S. Yurdakal, V. Augugliaro, RSC Adv. 2 (2012) 8375-8380.